Crystal-chemical reasons for the immiscibility of periclase and wüstite under lithospheric P, T condition

Article *in* European Journal of Mineralogy · September 2001

DOI: 10.1127/0935-1221/2001/0013/0871

CITATIONS
25

READS
290

5 authors, including:

Franca Caucia
University of Pavia Italy
37 PUBLICATIONS **399** CITATIONS

SEE PROFILE

Marcello Merli
Università degli Studi di Palermo
53 PUBLICATIONS **753** CITATIONS

SEE PROFILE

Eur. J. Mineral.
2001, **13**, 871–881

Dedicated to Prof. Dr. Wolfgang F. Müller
on the occasion of his 60th birthday

Crystal-chemical reasons for the immiscibility of periclase and wüstite under lithospheric P, T conditions

MASSIMO BOIOCCHI[1,2], FRANCA CAUCIA[1,2], MARCELLO MERLI[1,2], DANILO PRELLA[1,2] and LUCIANO UNGARETTI[1,2]

[1] Dipartimento di Scienze della Terra, Università di Pavia, via Ferrata 1, I-27100 Pavia, Italy
[2] CNR-Centro di Studio per la Cristallochimica e la Cristallografia (CSCC),
via Ferrata 1, I-27100 Pavia, Italy
e-mail: boiocchi@crystal.unipv.it

Abstract: We have analyzed the implications of $[Mg]^{VI}$=>$[Fe^{2+}]^{VI}$ isomorphous substitution in the periclase structure (B1) which forms, under lithospheric P, T conditions, only very limited solid solutions with wüstite. The crystallographic study (by single crystal X-ray structure refinements and microprobe analysis) supports the key role of the cation-cation repulsive interactions in the crystal-chemical behaviour of these closely-packed phases. The anomalously large octahedral bond lengths in periclase (Mg-O=2.106 Å) and in wüstite (Fe-O=2.167 Å) are the result of otherwise too short M-M distances (=1.414 · M-O). In particular, the wüstite instability below 570 °C and the problematic existence of a stoichiometric iron end-member indicate that the M-M separation in the "ideal" wüstite, although largely increased by the anomalously large Fe-O bond length, is still too short to support the B1 structure. Any periclase-wüstite solid solution with a wüstite component higher than 8.3 % necessarily entails the presence of couples of adjacent $[Fe^{2+}]^{VI}$ cations with separations shorter than that of "ideal" wüstite; this makes the solid solutions in this system even less stable than the pure wüstite. One easy way to reduce the electrostatic $[Fe^{2+}]^{VI}$-$[Fe^{2+}]^{VI}$ repulsion, and therefore the instability of iron-bearing periclase, is the iron oxidation with the formation of a more stable spinel phase (magnesioferrite), as it has been demonstrated by heat treatment and structure refinement of several natural ferropericlase crystals with 2-5 % of wüstite component. Magnesioferrite has a unit-cell edge of 8.39 Å which is almost twice the unit-cell of periclase (2 · 4.21 = 8.42 Å) and this allows the spinel to grow with the same orientation of periclase, being the oxygen arrangement of the two structures virtually identical. Under very high pressure (≥ 90 GPa) the electrostatic $[Fe^{2+}]^{VI}$-$[Fe^{2+}]^{VI}$ repulsion of FeO can be greatly reduced by a phase transition from B1 to B8 (NiAs) structure. In the B8 phase the Fe-Fe separation becomes 2.57 Å; this short value corresponds to a change in the electronic properties of iron which can now form metallic bonds, in contrast to MgO (B1) phase which is supposed to maintain its stability up to at least 230 GPa.

Key-words: periclase, wüstite, X-ray diffraction, heat treatment, repulsive interactions.

Introduction

The periclase-wüstite solid solution [(Mg,Fe)O] is believed to be an important component of Earth's mantle (Agee, 1998; Bina, 1998), where the high pressure phase transformation of the silicate spinel [ringwoodite, $(Mg,Fe)_2SiO_4$] produces silicate perovskite [$(Mg,Fe)SiO_3$] plus an oxide phase in the periclase-wüstite system. The post-spinel breakdown is assumed to contribute to the seismic discontinuities located at 660 km depth, and periclase-wüstite solid solutions are considered volumetrically significant phases (20 % by volume in a pyrolite mantle, according to Bina, 1998) in the lower mantle (660-2900 km). In the crust, periclase is a rare mineral and, when it forms, there is usually negligible or small (< 5 %) wüstite component. Periclase with the maximum amount of iron so far

DOI: 10.1127/0935-1221/2001/0013/0871
0935-1221/01/0013/0871 $ 2.75

found in nature (0.14 Fe atoms per formula unit, *apfu*) are diamond inclusions, suggesting an origin from ultradeep (>400 km) and highly reduced source regions (Haggerty, 1991). The lack of natural wüstite-rich solid solutions, although magnesium and iron are so abundant and ubiquitous, suggests that these oxide phases are unstable under the P, T conditions of formation of the accessible rocks.

The limited $Mg \Rightarrow Fe^{2+}$ substitution occurring in natural periclase contrasts with the ubiquitous abundance of solid solutions between $[Mg]^{VI}$ and $[Fe^{2+}]^{VI}$ end-members in the other common minerals, such as olivine, amphibole, pyroxene, etc. The occurrence of (Mg, Fe^{2+}) solid solutions is generally justified by the small difference between $[Mg]^{VI}$ and $[Fe^{2+}]^{VI}$ ionic radii and by their very similar bonding requirements.

In order to understand the reason for the great reluctance of periclase structure to host significant amounts of iron, at least at lithospheric P, T conditions, we have performed single-crystal refinements of synthetic MgO and of natural periclase with variable iron content (0.03-0.05 Fe *apfu*) so that we may compare bond distances, their variation with the iron content and possibly determine the exact iron location and its structural role.

Periclase crystal structure

Periclase crystallizes in the $Fm\bar{3}m$ space group (number 225) and its crystal structure (B1, *i.e.* NaCl-type) can be described as a cubic close-packing of oxygen atoms, with all the octahedral interstices (M) occupied by divalent cations and all the tetrahedral cavities (T) vacant. In the stoichiometric structure, each octahedron shares all twelve edges with twelve neighbouring octahedra. Oxygen is in six-fold coordination with the divalent cation which explains the relatively high density of end-members (3.58 g/cm^3 for periclase and 5.86 g/cm^3 for wüstite). The M, O and T sites are in special positions (with coordinates 000, ½½½ and ½½½, respectively); for this reason the structural geometric features are simple linear functions of the unit-cell edge a. Therefore, the nearest interatomic contacts, their values in Å (for $a = 4.211$ Å) and their multiplicity (m) are:

$$\text{M-O} = \frac{a}{2} = 2.106 \text{ Å}, \; m = 6;$$

$$\text{T-O} = \text{T-M} = a \cdot \frac{\sqrt{3}}{4} = 1.823 \text{ Å}, \; m = 4;$$

$$\text{M-M} = \text{O-O} = a \cdot \frac{\sqrt{2}}{2} = 2.978 \text{ Å}, \; m = 12.$$

All the coordination polyhedra are regular and identical, so that the M-O / T-O ratio must be:

$$\left(\frac{a}{2}\right) / \left(a \cdot \frac{\sqrt{3}}{4}\right) = \frac{2}{\sqrt{3}} = 1.155.$$

Each tetrahedral site, in the first neighbouring shell, has four oxygens and four cations at the same distance; consequently, if a T site would be occupied by a cation, four cationic vacancies must originate around it in order to decrease overbonding on the involved oxygens and to avoid short T-M contacts (1.823 Å).

Therefore the periclase structure offers only limited geometric flexibility; the only geometric variations which can occur are dependent upon isomorphous substitutions at the M site, which affect the M-O bond length and, consequently, the unit-cell edge and the M-M separation, the ratio between octahedral and tetrahedral bond distance remaining fixed at 1.155.

Experimental

Samples

The crystals studied in this work belong in part to the mineralogical collection of the Dipartimento di Scienze della Terra, University of Pavia, and in part to private collections. The synthesis conditions of pure MgO crystals (gem quality, colourless, here named "Per. synt") are unknown. Natural periclase (Monte Somma, Italy, here named "Per. 4041" and "Per. 3363") is in a paragenesis with a slightly magnesitic calcite ($Mg_{0.05}Ca_{0.95}CO_3$) and shows a distinct red-brown colour.

Five synthetic MgO crystals and twelve natural ferropericlase crystals have been used for microprobe analysis and for X-ray data collection and refinement.

X-ray diffraction

Periclase crystals were selected for X-ray data collection (Philips PW-1100 automated four-circle diffractometer) on the basis of their sharp diffraction profiles and of the optimal size required for collecting very high resolution data (~0.5 · 0.5 · 0.5 mm). Lattice constants have been calculated from least-squares refinement of the d values obtained, for 60 rows of the reciprocal lattice, by measuring the barycentre of each reflection and of its corresponding antireflection in the 2θ range between -70° and 70° (LAT routine of the PW-1100 soft-

ware). Intensity data were collected for all the reflections included within the 2θ range 3-134° with $\pm$ h, $\pm$ k, +l using the step-scan profile technique of Lehman & Larsen (1974) and ω-2θ scan mode. The intensity data (~ 680 measured reflections) were corrected for absorption (μ = 10.23 cm^{-1} for MgO; μ = 19.09 cm^{-1} for $Mg_{0.95}Fe_{0.05}O$) by the empirical method of North *et al.* (1968), and for Lorentz and polarization effects; after merging, 55 independent structure factors (F_{obs}) were obtained. The discrepancy factor between equivalent reflections (R_{sym}) is very low ($\leq$ 3.0 %) and no evidence of lower Laue symmetry has been obtained.

Structure refinement

The crystal structure was refined for all the samples in the space group $Fm\bar{3}m$ using the whole set of independent structure factors; a locally-modified version of the program ORFLS (Busing *et al.*, 1962) implemented by the weighting procedure of Spagna & Camalli (1999) has been used, with the weighting scheme "2" suggested by Cruickshank (1965). Model parameters include: scale factor, secondary extinction coefficient, occupancy of the O site (ionized *vs.* neutral scattering factors, with the total constrained to be 1.0), occupancy of the M site (Mg^{+2} *vs.* Fe^{2+} scattering factors, with the total constrained to be 1.0) and isotropic atomic thermal displacement (B_{iso}) for O and M sites. Owing to the very high resolution of the X-ray data (1.30 $Å^{-1}$), the correlation among the six model parameters was so low that they could all be refined in every least-squares cycle as independent variables (*e.g.* the correlation coefficient between occupancy and B_{iso} of the M site was always < 0.40). The refinements, carried out by using all the observed F values, converged to a very low discrepancy factor ($0.007 \leq R_{all} \leq 0.018$; $0.008 \leq R_w \leq 0.020$); in the case of the MgO crystals, the reflection (2 0 0), which has a low θ value and a very strong intensity, was excluded from the refinement in the last cycles. Final ΔF maps were calculated for all the samples.

SEM-WDS analyses

After X-ray data collection, the crystals were analyzed with a Jeol JXA 840A scanning electron-microscope equipped with a WDS analyser for Kα X-ray lines operating at 20 kV / 20 nA, using a gas flow (Ar90-$CH_4$10) proportional counter. The standards were pure pyrope for Mg, and natural almandine for Fe and Mn. Each crystal was analyzed at a minimum of 10 points and no chemical inhomogeneity was detected on this level. Analyses gave total oxide content very close to 100 %, with no significant presence of cations other than Mg and Fe. Small amounts of manganese (MnO $\leq$ 0.1 weight %) were detected in the natural ferropericlase samples.

Crystallographic results

The chemical analysis of one synthetic MgO crystal and of two natural ferropericlase crystals, with the lowest and the highest iron content (5.23 and 8.22 FeO weight %, respectively), are reported in Table 1. The refinement results of these three samples, which are thoroughly representative of the crystal-chemical behaviour of the 17 refined crystals, are reported in Table 2.

The M-occupancy of the five samples of pure MgO converged to a mean atomic number (*man*) of 11.97 ± 0.02 electrons, that is only slightly lower than the value corresponding to a full Mg-occupancy (12 electrons). The reason for this small, but systematic, deviation from the expected M-*man* was found to result from an incomplete extinction correction. By excluding from the least-squares procedure the reflection (2 0 0), characterized by a systematic negative F_o-F_c value, the octahedral occupancy converged in all cases to a M-*man* of 12 ± 0.02 electrons. The *a* value is in good agreement with that reported for pure periclase by Dubrovinsky & Saxena (1997). The final ΔF maps do not show any significant electron density residue. The isotropic atomic displacement parameters (B_{iso}) of M and O sites are very similar (Table 2); the B_{iso} of the O site is only slightly larger than that of M site, in agreement with the suggestions of Tsirelson *et al.* (1998).

Table 1. Microchemical analysis of three selected periclase crystals.

	Per.synt	Per.4041	Per.3363
weight %			
MgO	100.00 ± 6	93.94 ± 5	90.48 ± 5
FeO		5.23 ± 2	8.22 ± 3
MnO		0.04 ± 1	0.07 ± 1
Tot.	100.00	99.21	98.70
atoms per formula unit			
Mg	1.00	0.97	0.95
Fe^{2+}		0.03	0.05

Table 2. Structure refinement results of selected periclase crystals ($2\theta_{max}$=134°, Mo$K\alpha$).

	Per.synt	Per.4041	Per.3363
a (Å)	4.2113 (5)	4.2154 (5)	4.2178 (7)
R_{sym} (%)	1.40	2.50	1.90
R_{all} (%)	0.90	1.28	0.65
R_w (%)	1.27	1.55	0.83
G. of F.	0.94	0.74	0.89
F_{000} (e)	80.00	81.44	82.35
O site population	0.74 O^{2-} + 0.26 O	0.78 O^{2-} + 0.22 O	0.59 O^{2-} + 0.41 O
B_{iso} O (Å^2)	0.36 (1)	0.36 (1)	0.37 (1)
M site population	1.000 Mg^{2+}	0.974 Mg^{2+} + 0.026 Fe^{2+}	0.958 Mg^{2+} + 0.042 Fe^{2+}
M-*man* (e)	12.00 (2)	12.36 (2)	12.59 (2)
B_{iso} M (Å^2)	0.35 (1)	0.35 (1)	0.34 (1)
M-O (Å)	2.1056	2.1077	2.1089
M-M = O-O (Å)	2.9778	2.9807	2.9824
T-O = T-M (Å)	1.8235	1.8253	1.8264
Number of independent structure factors = 55.			

R_{sym} = conventional discrepancy factor between symmetry equivalent reflections;
R_{all}, R_w = conventional and conventional weighted disagreement index of the refinement;
G. of F.= goodness of fit = $[\Sigma w (F_o-F_c)^2 / (m-n)]^{1/2}$, m = number of observations, n = number of variables;
F_{000} = number of electrons in the unit cell; B_{iso} = isotropic atomic displacement parameter.

The refined M-occupancy for the twelve ferropericlase crystals was variable from crystal to crystal and showed a substantial scattering with the corresponding M-O bond length (Fig. 1). Moreover, the refinements showed a small but systematic deficit in the number of electrons in the M site, *i.e.* of octahedral iron, compared to the total iron content given by the corresponding chemical analysis. Furthermore, in all the final ΔF maps, some low electron density residual (2-3 times the background) was located at the tetrahedral site, but for many crystals it was not possible to refine the T-occupancy. When the T-occupancy refinement converged, its value was negligible (<0.02 electrons) and, therefore, it was not possible to reconcile the discrepancy with the chemical analysis (the deficit was ranging, for all refinements, between 0.06 and 0.35 electrons *p.f.u.*). Although very small, and practically not refinable, the electron density residue present in the T site and its relatively small dimension (T-O=1.826 Å) suggested that a small amount of trivalent iron could occupy the T site. This hypothesis was supported by the fact that, in all the syntheses of MgO-FeO solid solutions made so far (Jackson *et al.*, 1978; Bonczar & Graham, 1982; Srečec *et al.*, 1987; Waychunas *et al.*, 1994; Reichmann *et al.*, 2000) it was never possible to prevent the formation of trivalent iron. Even when syntheses were made under very reducing atmosphere (CO_2-H_2 Srečec *et al.*, 1987; Waychunas *et al.*, 1994) some Fe^{3+} always formed and its amount was increasing with increasing total iron content (Fig. 2). Moreover, some tetrahedral Fe^{3+} was spectroscopically detected by Waychunas (1983) in

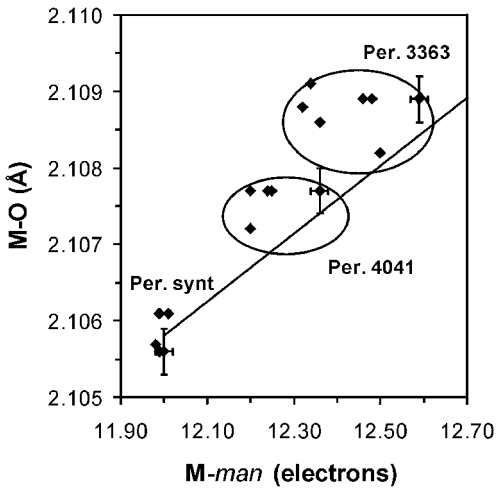

Fig. 1. Octahedral bond length variation *vs.* mean atomic number of the M site. The line connects the two stoichiometric end-members; the standard deviations, very similar for all the refinements, are shown only for the three selected samples of Table 2.

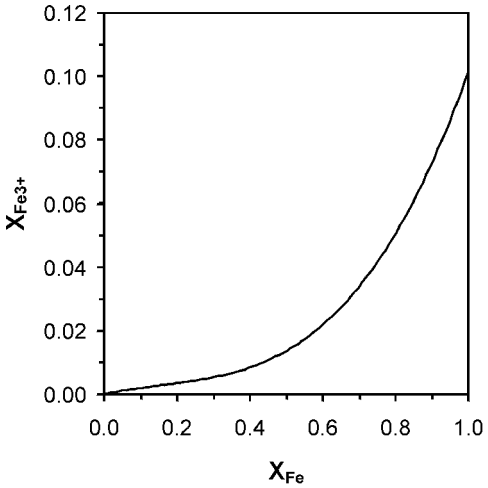

Fig. 2. Concentration of Fe^{3+} into synthetic periclase-wüstite solid solutions (from Srečec *et al.*, 1987). $X_{Fe3+} = Fe^{3+}/O$; $X_{Fe} = Fe/(Fe+Mg)$.

iron-poor synthetic periclase, although its structural role was not clear.

In conclusion, there are three main results from the crystallographic analysis which need to be explained:

1) some electron density in the tetrahedral site is present in all the final ΔF maps of the natural ferropericlase crystals; for many reasons this electron density residue could be associated with the presence of some trivalent iron, but it was never possible, by means of structure refinement, to determine with certainty its amount and its nature;

2) in all the natural periclase crystals, the iron content measured by microchemical analysis is always higher than that obtained by (M + T)-occupancy refinement;

3) there are variable M-*man* values for similar M-O, and therefore *a*, values (Fig. 1).

Heating experiments on natural periclase crystals

In order to cast light on the peculiar crystal-chemical features apparent in the refinement of natural periclase, we performed heating experiments on some of the studied single-crystals. The heating experiments were carried out in air in a temperature range between 300 and 1600 °C. After each heating, the crystal was quenched in an H_2O bath. With this treatment our main objectives were:

1) increasing the amount of trivalent iron (at the expense of the divalent iron) in order, hopefully, to be able to follow its localization;

2) allowing, by thermal expansion (Dubrovinsky & Saxena, 1997), some increase of the unit-cell edge and, consequently, some size increase of the tetrahedral cavity in order to favour its occupation by trivalent iron; the expected bond length for $[Fe^{3+}]^{IV}$-O is ~1.89 Å (Fleet, 1984), against a T-O value of only 1.826 Å in periclase;

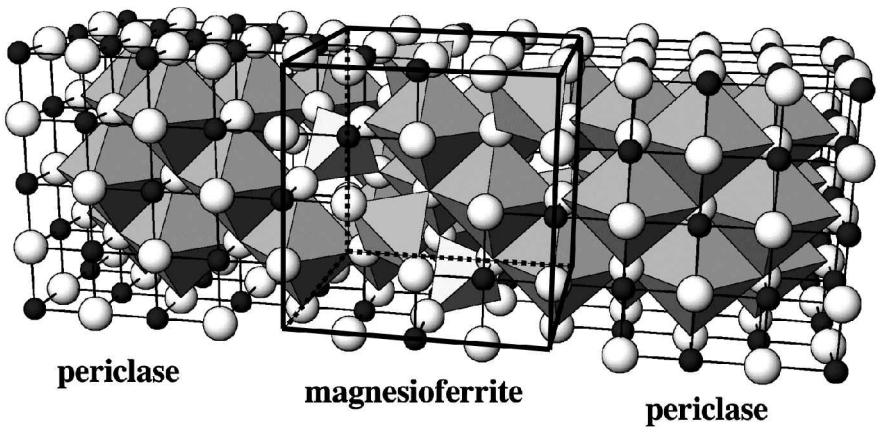

Fig. 3. A simplified drawing of syntaxial intergrowth of magnesioferrite in the periclase structure. The oxygen packing (light spheres) remains coherent between the two phases; the M sites (dark spheres) are totally occupied in periclase and half occupied in spinel, where 1/8 of the T cavities are populated and form isolated tetrahedra.

3) quenching-in the high-temperature structure.

The crystals heated above 900 °C showed a colour variation from red-brown to black and were characterized by strong magnetic properties. Mounting the heated crystals on the X-ray diffractometer, new reflections were found which were indexed according to an F-centred cubic unit cell with an edge double of that of periclase and with the same orientation. The high resolution crystal-structure refinement of the heated periclase samples allowed the detection of a significant amount of a spinel phase ($_{spin}$), with exactly the composition of magnesioferrite $MgFe_2O_4$, grown within the periclase ($_{peri}$) crystal. The structural analogy between these phases ($a_{peri} \approx 4.21$ Å, $a_{spin} \approx 8.39$ Å) allows their syntaxial intergrowth; the oxygen framework of periclase has to be only very slightly rearranged to become part of the structure of magnesioferrite (Fig. 3). It is possible to monitor the amount of spinel formed during the heat treatment by measuring the intensity of reflections with uneven indices, which are exclusive of the spinel phase [*e.g.* the strong reflection (3 1 1)]. It was discovered that these reflections (and therefore the spinel structure) were already present in all the natural crystals; however they have weak intensities and broad pro-

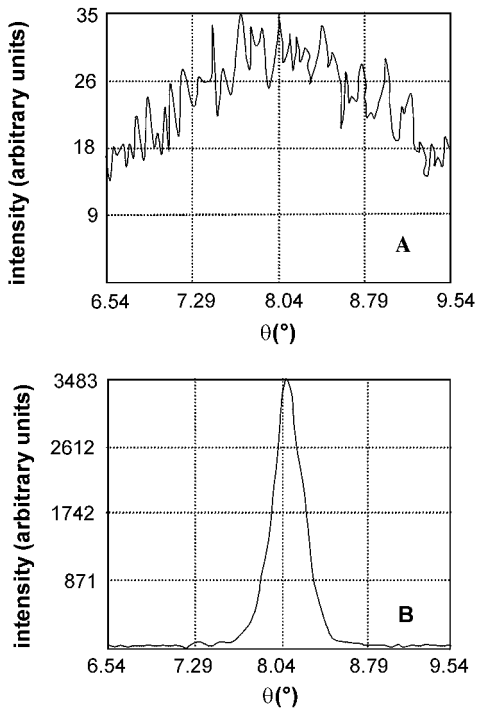

Fig. 4. Intensity of reflection (3 1 1) diffracted by a single crystal of natural periclase before (A) and after (B) a heat treatment at 1100 °C for 4 hours.

Table 3. Structure refinement of a periclase crystal (sample 3363) heated at 1100 °C and composed by a syntaxial intergrowth of periclase and magnesioferrite ($2\theta_{max}$=134°, Mo$K\alpha$).

3363 heated crystal	
R_{sym} (%)	2.10
R_{all} (%)	2.38
periclase fraction (%vol)	93.0 (1)
periclase	
a (Å)	4.212 (1)
F_{000} (e)	80.56
B_{iso} O (Å^2)	0.36 (1)
M site population	0.99 Mg^{2+} + 0.01 Fe^{2+}
M-*man*(e)	12.14 (2)
B_{iso} M (Å^2)	0.35 (1)
M-O (Å)	2.106 (1)
composition	$Mg_{0.99}$ $Fe^{2+}{}_{0.01}$ O
magnesioferrite	
a (Å)	8.385 (2)
F_{000} (e)	764.48
u	0.2566 (3)
$B_{eq.}$ O (Å^2)	0.51 (4)
M site population	0.37 Mg^{2+} + 0.63 Fe^{3+}
M-*man* (e)	20.87 (15)
$B_{eq.}$ M (Å^2)	0.48 (1)
T site population	0.30 Mg^{2+} + 0.70 Fe^{3+}
T-*man* (e)	21.82 (15)
$B_{eq.}$ T (Å^2)	0.43 (1)
M-O (Å)	2.042 (2)
O-M-O (°)	86.83 (10)
T-O (Å)	1.912 (2)
x	0.70
composition (Tsite),	($Mg_{0.30}$ $Fe^{3+}{}_{0.70}$)
[M site]	[$Mg_{0.73}$ $Fe^{3+}{}_{1.27}$] O_4

Overall composition of the crystal based on 1 oxygen *pfu*:
0.93 · (0.99 Mg + 0.01 Fe^{2+}) +
+ 0.07 · (1.03/4 Mg + 1.97/4 Fe^{3+}) =
Mg 0.939 + Fe^{2+} 0.009 + Fe^{3+} 0.034 =
91.84% MgO + 1.57% FeO + 6.59% Fe_2O_3.

Number of independent structure factors = 302.

Legend as in Table 2; u = atomic fractional coordinate of oxygen; O-M-O = octahedral bond angle; x = spinel inversion parameter; $B_{eq.}$ = equivalent isotropic thermal displacement.

X-ray data collection necessary to refine both periclase and spinel phases has been performed in a cubic unit cell with *a*=8.42 Å; after the data collection, the unit cell edge of periclase has been calculated from the least-squares refinement of reciprocal rows (LAT procedure) with h, k, l, even (*i.e.* the reflections belonging only to the spinel have been excluded); the unit cell edge of magnesioferrite has been calculated from LAT procedure of reciprocal rows belonging only to the spinel phase (with h, k, l odd).

files (Fig. 4A) so that they are not detectable in the standard peak-hunting procedure.

After heating the periclase crystals at 1100 °C for 4 to 5 hours, the intensity of reflection (3 1 1) reaches its maximum value (Fig. 4B), indicating that no further oxidation can be achieved. X-ray diffraction data (up to resolution of 1.30 $Å^{-1}$) of the heated crystals were collected in a cubic cell with a = 8.42 Å and the crystal structures of periclase and spinel, and their proportion, were obtained by means of a special least-squares procedure. As far as the spinel phase is concerned, the oxygen atomic coordinate (u), the M and T occupancy and the equivalent isotropic atomic thermal displacement (B_{eq}) for all the atomic sites were refined (Table 3). The results show that virtually all the iron originally present in the periclase crystal is now oxidized giving rise to magnesioferrite, and that periclase becomes practically pure. Unconstrained site-occupancy refinement of magnesioferrite gave an almost stoichiometric composition in perfect agreement with the refined bond length values. The inversion parameter (x) of magnesioferrite is in good agreement with the value estimated in the literature for these experimental conditions ($0.71<x<0.73$, O'Neill *et al.*,1992). The overall composition of intergrown periclase and magnesioferrite (respectively 93 % and 7 % by volume), obtained from the chemically unconstrained refinement of the heated crystal reported on Table 3, is in good agreement with the microprobe analysis of the 3363 natural crystal reported on Table 1.

The spinel occurs predominantly along the rim of periclase crystal; in this region a great number of precipitates appear (Fig. 5) which correspond to magnesioferrite domains, all having the same orientation of the original ferropericlase crystal. The macroscopic features showed by the heated crystals are in agreement with those reported in the literature (Ricoult & Schmalzried, 1987).

The spinel phase remains stable at T ≤ 1200 °C; above this temperature its amount decreases progressively and at T = 1600 °C all the magnesioferrite domains disappear. Very likely the magnesioferrite domains melt so that the iron reacts with the platinum crucible leaving a crystal of pure colorless periclase.

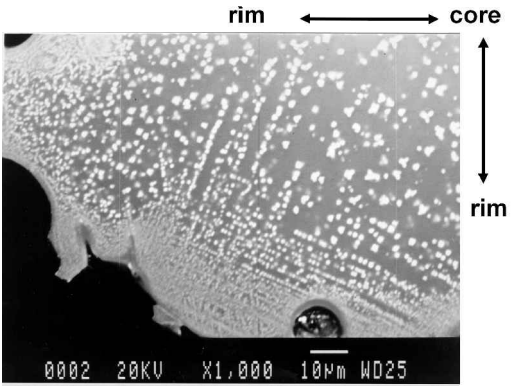

Fig. 5. Scanning electron micrograph of a periclase crystal heated at 1100 °C for 4 hours; the spinel precipitates appear as white dots.

Discussion

In Table 4 some crystallographic properties of the periclase and wüstite end-members are reported. It has to be noted that a stoichiometric wüstite has never been found in nature and that also its synthesis is very problematic because of the easy oxidiation of the iron; in fact, only two authors (Katsura *et al.*, 1967 and Hentschel, 1970) have claimed so far the synthesis of a stoichiometric wüstite, although with slightly different unit cell edge (4.323 ± 0.001 and 4.333 ± 0.001 Å, respectively). The values for wüstite reported in Table 4 refer to the ideal end-member and have been obtained by extrapolation (McCammon & Liu, 1984).

The Mg-O bond length in periclase (2.106 Å) is the largest so far found for magnesium with regular or almost regular octahedral coordination. The value of 2.106 Å has to be compared with the Mg-O distance of 2.078 Å which characterizes the octahedral sites in the most common rock-forming minerals, *e.g.* amphiboles (Hawthorne, 1983) and orthopyroxenes (Domeneghetti *et al.*, 1995). The anomalously large octahedral size of the M site in periclase is even more exaggerated in wüstite. In fact,

Table 4. Crystallographic properties of periclase and wüstite.

	periclase (MgO)	wüstite (FeO)[1]
a (Å)	4.211	4.334
unit cell vol.($Å^3$)	74.67	81.41
Z	4	4
density (g/cm^3)	3.58	5.86
M-O (Å)	2.106	2.167
octahedral vol.($Å^3$)	12.45	13.57
T-O = T-M (Å)	1.824	1.877
tetrahedral vol.($Å^3$)	3.11	3.39
M-M = O-O (Å)	2.978	3.065

[1] =values extrapolated by McCammon & Liu, 1984.

Legend as in Table 2.

going from periclase to wüstite, we observe an octahedral length variation from 2.106 to 2.167 Å and, therefore, an octahedral bond increase of 0.061 Å, a value significantly greater than the typical value of 2.120 – 2.078 = 0.042 Å shown, for instance, by the octahedral sites of amphiboles; likewise 0.042 Å is the octahedral bond difference between magnesite and siderite end members (Effenberger *et al.*, 1981). The value of 0.042 Å, that occurs with negligible variations in several femic rock-forming minerals, can be assumed as the true ionic radius difference between $[Mg]^{VI}$ and $[Fe^{2+}]^{VI}$ cations in the absence of strong structural geometric constraints. It has to be noted that the revised effective ionic radii of $[Mg]^{VI}$ (0.72 Å) and $[Fe^{2+}]^{VI}$ (0.78 Å; Shannon, 1976) give a difference of 0.06 Å; however, in rock-forming minerals without structural constraints, such a large difference has never been found. Therefore, the anomalous Mg-O bond length in periclase (2.106 instead of the more common 2.078 Å) and the still higher value of Fe-O in wüstite (2.167 instead of the more common 2.120 Å) must be the result of some structural constraint, which can only be found in the short separation between next-nearest identical atoms (O-O = M-M = 1.414 · M-O). The O-O distance is in the range of values commonly found in minerals, so the M-M separation has to be responsible for the increase of the M-O length. Thus, in these closely-packed phases, the non-bonding requirements of the cations (the non-bonded radii of O'Keeffe & Hyde, 1981) are the dominant aspects of the structural geometry and, consequently, are able to affect significantly the bond distances.

It should also be considered that the Mg-Mg separation in periclase (2.978 Å) is one of the shortest values so far found and that this value has been obtained by forcing the Mg-O distance to reach the largest value among the $(MgO)^{VI}$-bearing compounds. However, since it is relatively easy to synthesize MgO as a stable phase, a value of 2.106 Å for Mg-O bond length and a Mg-Mg separation of 2.978 Å still clearly fits the stability requirements of the structure. On the contrary, the Fe-Fe distance of 3.065 Å in the extrapolated ideal wüstite, although obtained by forcing the Fe-O bond length to reach the largest value so far found (2.167 Å), is evidently still too short, as indicated by the extreme difficulty of synthesizing a stoichiometric phase. With the more common $[Fe^{2+}]^{VI}$-O value of ~ 2.12 Å, the Fe-Fe separation in wüstite would be so short (~ 3 Å) to make impossible its crystallization.

The strong electrostatic repulsion between adjacent iron cations is therefore responsible for instability of wüstite and for its transformation into magnetite + Fe at T < 570 °C and one atmosphere (Lindsley, 1991). It also explains the impossibility of synthesizing wüstite with even a small periclase component and the occurrence, in nature, of periclase with just a limited wüstite component. Actually, substitution of magnesium for iron into wüstite would decrease the octahedral bond length, according to the lower ionic radius of magnesium; consequently the unit-cell edge and the M-M distances in a periclase-wüstite solid solution would decrease in respect to the corresponding values in wüstite. Since the Fe-Fe contact in wüstite is at a limiting value for pairs of divalent iron atoms, its further reduction by substitution of Fe^{2+} by Mg is not possible. On the other hand, a limited substitution of Mg by Fe^{2+} may occur in periclase, because it slightly expands the structure reducing the cation-cation repulsion. Obviously, the extent of the substitution is limited by the necessity of avoiding the formation of adjacent Fe^{2+}-Fe^{2+} pairs. When the iron occupancy at the M site of periclase exceeds 1/12 of the total occupancy (*i.e.* 0.083 Fe-*apfu*) it is impossible to prevent the formation of Fe^{2+}-Fe^{2+} pairs at a distance which is significantly shorter than that occurring in wüstite; the resulting very strong electrostatic repulsion between adjacent iron atoms would prevent the formation of solid solutions with these compositions.

Only under high temperature conditions, with an increase of the M-M separation because of the thermal expansion, does it become possible to stabilize ferropericlase with iron content greater than 0.083 Fe-*apfu*. However, under lithospheric conditions, these iron-rich compositions transform into an almost pure periclase and a less dense phase, the spinel structure, characterized by atomic sites with lower coordination number (oxygens in four-fold coordination; half octahedral sites occupied and half vacant; 1/8 of the tetrahedral sites occupied) and much lower cation-cation repulsion (as indicated by the presence of cation-oxygen bond lengths of standard value). This, at least in part, may explain the widespread natural occurrence of spinel and the absence in the lithosphere of iron-rich periclase-wüstite solid solutions.

Conclusions

We have seen that cation-cation repulsive forces are responsible for the instability of periclase-wüstite solid solutions, at least under lithospheric P, T conditions. Most important is the electrostatic Fe^{2+}-Fe^{2+} repulsion occurring in wüstite, which becomes

even stronger in ferropericlase. Under high oxygen fugacity the strong cation-cation repulsive interaction can be reduced by oxidizing the divalent octahedral iron. In this way ferropericlase transforms into almost pure periclase and the oxidized iron can now enter 1/8 of the vacant tetrahedral sites of periclase giving rise to a spinel phase.

We have shown that this spinel phase has the composition of magnesioferrite and the same oxygen arrangement and orientation of periclase. This is made possible by the virtual coincidence of the oxygen framework in the two structures, as indicated by the great coherence of their unit cells (8.39 Å for magnesioferrite and $2 \cdot 4.21 = 8.42$ Å for periclase). In other words, the growth of magnesioferrite is simply obtained by adding oxygen and shifting the oxidized iron to the vacant tetrahedral sites, leaving the remaining periclase structure almost unchanged. It has to be noted that the T site of periclase is characterized by a T-O bond length (~ 1.82 Å) which is too short for any of the available cations. With the small rearrangement of the oxygen framework required to form magnesioferrite, the T-O bond length increases up to a value (~ 1.91 Å) which is now perfectly suitable for the T-site population obtained by the refinement.

Some syntaxial spinel component has been found in all of the crystals of natural ferropericlase that we have examined. This allows us to explain the three main crystallographic results obtained by the refinement of the natural ferropericlase crystals. The electron density residue seen in the ΔF maps in the tetrahedral cavity is due to the small amounts of syntaxial magnesioferrite. However, the T-occupancy refinement was unsuccessful because the measured reflections were only those indexed with the periclase unit-cell (merged to 55 F_{obs}). Consequently, most of the reflections necessary to refine the T-occupancy, and precisely those belonging only to the spinel phase ($302 - 55 = 247$ F_{obs}), were not collected. Similarly, the 55 F_{obs} collected to refine periclase cannot give correct results because they are inevitably affected by the presence of syntaxial spinel, in which 1/2 of the octahedral sites are vacant. Therefore, the M-vacancy of the spinel phase affects the refined M-*man* of periclase which, necessarily, is underestimated according to the amount of intergrown magnesioferrite. Finally, due to the strong structural analogies between periclase and spinel, the presence of variable amounts of the latter does not produce significant variation of the *a* value which remains unchanged for all the crystals coming from the same sample; therefore, the refined M-*man* values of ferropericlase crystals deviate from the line shown in Fig. 1 according to their spinel content.

The presence of some spinel phase in all the studied natural samples suggests that, at least under lithospheric P, T conditions, iron-bearing periclase is unstable and spontaneously transforms into a peculiar two-phase assemblage (periclase and magnesioferrite) in which the amount of magnesioferrite depends upon the amount of iron which is oxidized.

Quite different is the situation occurring in wüstite which is always characterized by a marked nonstoichiometry due to a partial iron oxidation occurring even under very reducing atmosphere. Several different hypotheses have been proposed about the arrangement of point defects in wüstite, with clusters of octahedral vacancies and tetrahedral occupied sites having different size according to P, T, fO_2 or other experimental conditions (Catlow, 1981; Sørensen, 1981; Welberry & Christy, 1997; Minervini & Grimes, 1999). Very likely the instability of wüstite can be greatly reduced by the formation of a defect structure which, more or less quickly, evolves towards the formation of a spinel phase (magnetite). The wüstite-magnetite transformation is, at least in part, made difficult by the significant difference in the geometry of the oxygen framework of the two phases ($2\ a_{wüs} = 8.67$ Å to be compared with $a_{mag} = 8.39$ Å). The geometrical misfit between wüstite and magnetite makes highly improbable a coherent coexistence of the two phases, as it happens with the periclase-magnesioferrite pair. Therefore, the energetics of the process forming a spinel phase from ferropericlase or from magnesiowüstite is not the same and the process very likely will follow different crystal-chemical patterns.

Periclase and wüstite are also very different in their behaviour under very high pressure. MgO is supposed to maintain the B1 structure up to at least 230 GPa (Duffy *et al.*, 1995), whereas FeO exhibits complex polymorphism under pressure, with a major phase transition occurring at $P \geq 90$ GPa and $T = 873$ °C (Mao *et al.*, 1996). In particular, as shown by in situ high-P, high T X-ray diffraction ($P = 96$ GPa, $T = 1073$ °C; Fei & Mao, 1994), the B1 structure of FeO changes to a B8 (NiAs-type) distorted hexagonal closest-packed analogue. In the B8 structure the nearest neighbour Fe-Fe distances are much shorter (2.57 Å) than in wüstite, indicating an FeO transition from an ionically bonded structure to a strongly covalent and metallic one (Mazin *et al.*, 1998).

In conclusion the non-bond requirements of the cations explain the poor miscibility, under litho-

spheric P, T conditions, between isomorphous closely-packed phases characterized by strong repulsive interactions (not only between periclase and wüstite but also between corundum and hematite). On the contrary, complete miscibility between isomorphous end-members can easily occur when their structure does not have short intercation separations. A clear example of complete miscibility between Mg and Fe end-members is that offered by the magnesite-siderite series, which forms a complete solid solution along their join (manuscript in preparation); in this structure, although characterized by a dense oxygen packing, the octahedra do not share edges, remaining at a sufficient distance (> 3.6 Å) to avoid any repulsive interaction.

Acknowledgements: We are grateful to Dr. A. Callegari for his help in the microchemical analysis and for the electron micrographs of heated periclase crystals; G. Toscani is thanked for his continuous care in keeping our computing facilities operating always at the best level; we are much indebted with Prof. F. Mazzi for his refinement program able to deal with "syntaxial" crystals. Special thanks are due to M. Novaga and R. Pagano who provided some of the studied periclase samples. The precious suggestions and corrections by R. Angel and S. Jacobsen greatly improved and clarified the manuscript. This study was financially supported by the Ministero dell'Università e della Ricerca Scientifica e Tecnologica: project "Materiali terrestri ed analoghi di sintesi ad alta pressione ed alta temperatura: proprietà fisiche, chimiche e reologiche".

References

Agee, C.B. (1998): Phase transformations and seismic structure in the upper mantle and transition zone. *in* "Ultrahigh-pressure mineralogy: physics and chemistry of the earth's deep interior", R. J. Hemley, ed., *Rev. Mineral.*, **37**, 165-204.

Bina, C.R. (1998): Lower mantle mineralogy and the geophysical perspective. *in* "Ultrahigh-pressure mineralogy: physics and chemistry of the earth's deep interior", R. J. Hemley, ed., *Rev. Mineral.*, **37**, 205-240.

Bonczar, L.J. & Graham, E.K. (1982): The pressure and temperature dependence of the elastic properties of polycrystal magnesiowüstite. *J. Geophys. Res.*, **87**, 1061-1078.

Busing, W.R., Martin, K.O., Levy, H.A. (1962): ORFLS, a FORTRAN crystallographic least-squares program. Report ORNL-TM-305. Oak Ridge Nat. Labor, Tennessee.

Catlow, C.R.A. (1981): Defect clustering in nonstoichiometric oxides. *in* "Nonstoichiometric oxides", O.T. Sørensen, ed., Academic Press, New York, 61-99.

Cruickshank, D.W.J. (1965): Computing methods in crystallography. Oxford Pergamon Press, pp. 112-116.

Domeneghetti, M.C., Molin, G.M., Tazzoli, V. (1995): A crystal-chemical model for Pbca orthopyroxene. *Am. Mineral.*, **80**, 253-267.

Dubrovinsky, L.S. & Saxena, S.K. (1997): Thermal expansion of periclase (MgO) and Tungsten (W) to melting temperatures. *Phys. Chem. Minerals*, **24**, 547-550.

Duffy, T.S., Hemley, R.J., Mao, H.K. (1995): Equation of state and shear strength at multimegabar pressures: magnesium oxide to 227 GPa. *Phys. Rev. Lett.*, **74**, 1371-1374.

Effenberger, H., Mereiter, K., Zemann, J. (1981): Crystal structure refinements of magnesite, calcite, rhodocrosite, siderite, smithsonite, and dolomite, with discussion of some aspects of the stereochemistry of calcite type carbonates. *Z. Kristall.*, **156**, 233-243.

Fei, Y. & Mao, H. K. (1994): In situ determination of the NiAs phase of FeO at high pressure and temperature. *Science*, **266**, 1668-1680.

Fleet, M.E. (1984): The structure of magnetite: two annealed natural magnetites, $Fe_{3.005}O_4$ and $Fe_{2.96}Mg_{0.04}O_4$. *Acta Cryst.,* **C 40**, 1491-1493.

Haggerty, S.E. (1991): Oxide Mineralogy of the Upper Mantle. *in* "Oxide minerals: petrologic and magnetic significance", D. H. Lindsley, ed., *Rev. Mineral.*, **25**, 355-416.

Hawthorne, F.C. (1983): The crystal chemistry of the amphiboles. *Can. Mineral.*, **21**, 173-480.

Hentschel, B. (1970): Stoichiometrich FeO as metastable intermediate of the decomposition of wüstite at 225° C. *Z. Naturforsch.*, **25**, 1996-1997.

Jackson, I., Liebermann, R.C., Ringwood, A.E. (1978): The elastic properties of $(Mg_xFe_{1-x})O$ solid solutions. *Phys. Chem. Minerals*, **3**, 11-31.

Katsura, T., Iwasaki, B., Kimura, S., Akimoto, S. (1967): High-pressure synthesis of the stoichiometric compound FeO. *J. Chem. Phys.*, **47**, 4559-4560.

Lehman, M.S. & Larsen, F.K. (1974): A method for location of the peaks in step-scan-measured Bragg reflections. *Acta Cryst.*, **A30**, 580-586.

Lindsley, D.H. (1991): Experimental studies of oxide minerals. *in* "Oxide minerals: petrologic and magnetic significance", D. H. Lindsley, ed., *Rev. Mineral.*, **25**, 69-106.

Mao, H.K., Shu, J., Fei, Y., Hu, J., Hemley, R.J. (1996): The wüstite enigma. *Phys. Earth Planet. Int.*, **96**, 135-145.

Mazin, I.I., Fei, Y, Downs, R., Cohen, R. (1998): Possible polytypism in FeO at high pressures. *Am. Mineral.*, **83**, 451-457.

McCammon, C.A. & Liu, L. (1984): The effect of pressure and temperature on nonstoichiometric wüstite, Fe_xO: the iron-rich phase boundary. *Phys. Chem. Minerals*, **10**, 106-113.

Minervini, L. & Grimes, R. W. (1999): Defect clustering in wüstite. *J. Phys. Chem. Solids*, **60**, 235-245.

North, A.C.T., Phillips, D.C., Mathews, F.S. (1968): A semi-empirical method of absorption correction. *Acta Cryst.*, **A24**, 351-359.

O'Keeffe, M. & Hyde, B.G. (1981): The role of nonbonded forces in crystals. *in* "Structure and bonding in crystals I", M. O'Keeffe & A. Navrotsky, eds., Academic Press, New York, 227-254.

O'Neill, H. St. C., Annersten, H., Virgo, D. (1992): The temperature dependence of the cation distribution in magnesioferrite ($MgFe_2O_4$) from powder XRD structural refinements and Mössbauer spectroscopy. *Am. Mineral.*, **77**, 725-740.

Reichmann, H.J., Jacobsen, S.D., Mackwell, S.J., McCammon, C.A. (2000): Sound wave velocities and elastic constants for magnesiowüstite using gigahertz interferometry. *Geophys. Res. Lett.*, **27**, 799-802.

Ricoult, D.L. & Schmalzried, H. (1987): Internal reactions in the (Mg,Me)O system. *J. Mater. Sci.*, **22**, 2257-2266.

Shannon, R.D. (1976): Revised effective ionic radii and systematic studies of interatomic distances in halides and chalcogenides. *Acta Cryst.*, **A32**, 751-767.

Sørensen, O.T. (1981): Thermodynamics and defect structure of nonstoichiometric oxides. *in* "Nonstoichiometric oxides", O.T. Sørensen, ed., Academic Press, New York, 1-59.

Spagna, R. & Camalli, M. (1999): Analysis of weighting schemes. *J. Appl. Cryst.*, **32**, 934-942.

Srečec A.E., Ender, a., Woermann, E., Gans, W., Jacobsson, E., Eriksson, G., Rosén, E. (1987) Activity-composition relations of magnesiowüstite solid solution series in equilibrium with metallic iron in the temperature rage 1050-1400 K. *Phys. Chem. Minerals*, **14**, 492-498.

Tsirelson, V.G., Avilov, A.S., Abramov, Y.A., Belokoneva, E.L., Kitaneh, R., Feil, D. (1998): X-ray and electron diffraction study of MgO. *Acta Cryst.*, **B54**, 8-17.

Waychunas, G.A. (1983): Mössbauer, EXAFS and X-ray diffraction study of Fe^{3+} clusters in MgO:Fe and magnesiowüstite $(Mg,Fe)_{1-x}O$: Evidence for specific cluster geometries. *J. Mater. Sci.*, **18**, 195-207.

Waychunas, G.A., Dollase, W.A., Ross II, C.R. (1994): Short-range order measurement in MgO-FeO and $MgO-LiFeO_2$ solid solutions by DLS simulation-assisted EXAFS analysis. *Am. Mineral.*, **79**, 274-288.

Welberry, T.R. & Christy, A.G. (1997): Defect distribution and the diffuse X-ray diffraction pattern of wüstite, $Fe_{1-x}O$. *Phys. Chem. Minerals*, **24**, 24-38.

Received 31 March 2000
Modified version received 8 January 2001
Accepted 29 March 2001